



# Growth of transparent $\text{SrB}_4\text{O}_7$ single crystal and its new applications

Ryuichi Komatsu<sup>a,\*</sup>, Hiroaki Kawano<sup>a</sup>, Zenta Oumaru<sup>a</sup>,  
Keiji Shinoda<sup>b</sup>, Valentin Petrov<sup>c</sup>

<sup>a</sup>*Yamaguchi University, 2-16-1 Ube, Yamaguchi 755-8611, Japan*

<sup>b</sup>*Osaka City University, 3-3-138 Sugimoto, Sumiyoshi, Osaka 558-8585, Japan*

<sup>c</sup>*Max-Born-Institute for nonlinear optics and ultrafast spectroscopy, 2A Max-Born-Strasse, D-12489 Berlin, Germany*

Available online 9 December 2004

## Abstract

High-quality and transparent  $\text{SrB}_4\text{O}_7$  single crystal has been successfully grown by the Czochralski (CZ) method. Transparency from 200 to 1100 nm and dielectric changes with the temperature ranging from 300 to 750 K are measured. Crystal quality is discussed for second harmonic generation in VUV.  $\text{Sm}^{2+}:\text{SrB}_4\text{O}_7$  crystal has also been grown by the CZ method. Fluorescence line of  $\text{Sm}^{2+}$  close to 685.5 nm in a crystal is measured. It is revealed that  $\text{Sm}^{2+}:\text{SrB}_4\text{O}_7$  crystal is a promising material for a pressure gauge in a diamond anvil.

© 2004 Elsevier B.V. All rights reserved.

PACS: 81.10.Fq; 42.70.Mp; 78.55.Hx

Keywords: A2. Czochralski method; B1. Borate; B2. Fluorescence materials; B2. Nonlinear optic materials

## 1. Introduction

Piezoelectric crystals are used for surface acoustic wave (SAW) and nonlinear optical devices in electronic and communication equipment, such as mobile telephones, televisions and solid-state lasers. With the rapid advance in information technology, there have been strong and continuing

demands for improved functionality of these devices. One of the most critical issues in advancing this technology is to develop new piezoelectric crystals. Many efforts have been made to find new piezoelectric materials [1,2].

$\text{SrB}_4\text{O}_7$  crystal (SBO) is a piezoelectric material that belongs to the  $\text{Pnm}2_1$  space group and has unit cell parameters  $a = 4.4255 \text{ \AA}$ ,  $b = 10.709 \text{ \AA}$ ,  $c = 4.231 \text{ \AA}$ , and  $Z = 2$  [3]. Oseledchik et al. [4] reported the crystal growth of SBO crystal by the Cz method, whereas Fan et al. [5] reported the crystal growth by the Kyropoulos method. One of

\*Corresponding author. Fax: + 81 836 859631.

E-mail address: [r-komats@yamaguchi-u.ac.jp](mailto:r-komats@yamaguchi-u.ac.jp)  
(R. Komatsu).

most serious and common problems in borate crystal growth is the macroscopic opaque defect, in which the crystal becomes clouded [6].

Applications of SBO have been investigated since 1985 [7] and SBO has been attracting much attention as a nonlinear optical crystal with the following benefits: a transparency down to 120 nm, a high nonlinear coefficient, the highest damage threshold, and no hygroscopicity [3]. Komatsu and Ikeda [8] demonstrated that this crystal also had the highest SAW velocity among piezoelectric crystals. Recently, Petrov, one of the authors, reported the wavelength conversion of femtosecond SHG pulses down to 125 nm using SBO [9]. SBO is an attractive crystal for generating SHG pulses in the VUV region. However, crystals used in this study exhibited a different transmission. If a transparent crystal was used, valuable information, including precise SHG properties, were obtained. Thus, high-quality transparent crystals are required to determine precise SHG properties and to generate shorter pulses.

$\text{Sm}^{2+}$ :SBO has also gained attention as a pressure gauge in a diamond anvil that can generate extremely high pressure, up to 200 GPa. The shift of the fluorescence line (685.5 nm) of  $\text{Sm}^{2+}$  in this crystal was used to determine the pressure. This shift is almost unaffected by temperature. This establishes  $\text{Sm}^{2+}$ :SBO as a superior pressure gauge material, compared to ruby and other gauge materials. An individual researcher using a diamond anvil produced  $\text{Sm}^{2+}$ :SBO polycrystals from the melt in slow cooling. Crystal size in this polycrystal is very small (only up to 10  $\mu\text{m}$ ). This also includes other phases such as  $\text{SrB}_6\text{O}_{10}$  and  $\text{SrB}_2\text{O}_4$ , and exhibits variations in fluorescence intensity and a broader line width leading to uncertain results. To solve this problem, we paid attention to the  $\text{Sm}^{2+}$ :SBO crystal because this crystal has uniform properties compared to polycrystals. After studying the growth of the  $\text{Sm}^{2+}$ :SBO crystal, we determined that the precise pressure choice is possible if crystal is used instead of polycrystal. P Mikhail et al. [10] reported the growth of  $\text{Sm}$ :SBO single crystals using the Cz method. However, they did not investigate the application of grown crystal to a pressure gauge.

In this study, we describe the growth of high-quality SBO crystals, and  $\text{Sm}^{2+}$  bearing SBO crystals for the above two applications. We also discuss new measurement results required for these applications.

## 2. Experimental procedure

SBO and  $\text{Sm}^{2+}$ :SBO crystals were grown in air by the CZ method. The starting material comprised of SBO polycrystalline powder with the molar ratio (B/Sr) of 4.00 for SBO crystal growth.  $\text{SrB}_4\text{O}_7$  powder was prepared through solid–solid reaction of  $\text{SrCO}_3$  (99.9%),  $\text{H}_3\text{BO}_3$  (99.9%) or  $\text{B}_2\text{O}_3$  (99.9%) at 900 °C for 10 h. The pulling direction was parallel to  $\langle 010 \rangle$ , and growth and rotation rates were 0.1–0.3 mm/h and 5–20 rpm. Platinum (Pt) crucible used was  $50\phi \times 50$  mmh. The transparency at wavelengths from 190 to 1000 nm (Shimazu UV160) and the dielectric constant were measured over a wide temperature range of 300–750 K (HP 4284A).

$\text{SrB}_4\text{O}_7$  powder with  $\text{Sm}_2\text{O}_3$  (2, 5 wt%) added, was used as the starting material for  $\text{Sm}^{2+}$ :SBO crystal growth. Growth parameters are the same as above. The Sm content in grown crystals was measured by EPMA. The fluorescence spectra of grown crystal were also measured at room temperature by irradiation of an  $\text{Ar}^+$  laser (488 nm, 10 mW) onto a polished thin section ( $3 \times 3 \times 1$  mm<sup>3</sup>) made from grown crystals. The fluorescence intensity of 685.5 nm was then compared with that of  $\text{Sm}$ :SBO glass and  $\text{Sm}$ :SBO polycrystal made from the melt.

## 3. Results and considerations

### 3.1. Growth of transparent SBO single crystal

Fig. 1 shows a grown, cloudy SBO crystal. As shown in Fig. 2, microscopic observation revealed many inclusions in the cloudy crystals. Inclusions consist of voids and other phase material. Inclusions in borate crystals were caused by volatile impurities, such as water and by the deviation from the stoichiometric composition in the starting



Fig. 1. As-grown cloudy  $\text{SrB}_4\text{O}_7$  single crystal.

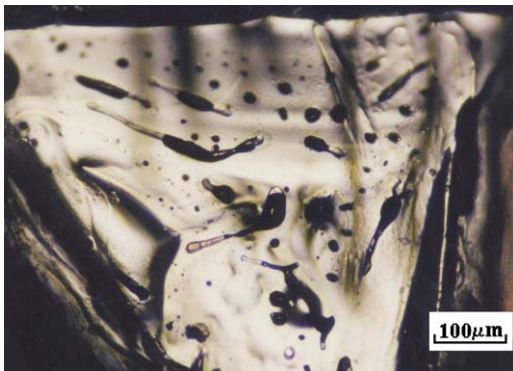


Fig. 2. Inclusions in cloudy  $\text{SrB}_4\text{O}_7$  crystal.

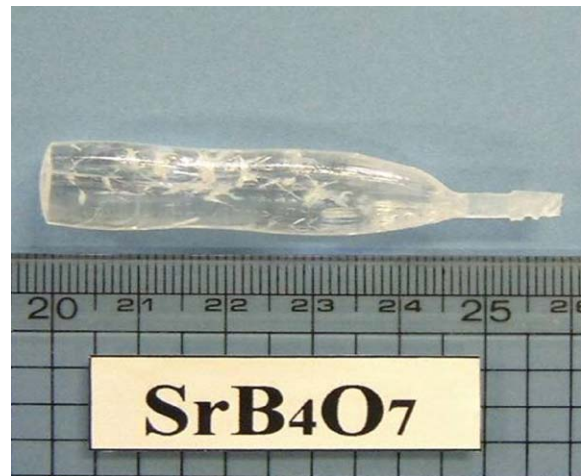


Fig. 3. As-grown transparent  $\text{SrB}_4\text{O}_7$  single crystal.

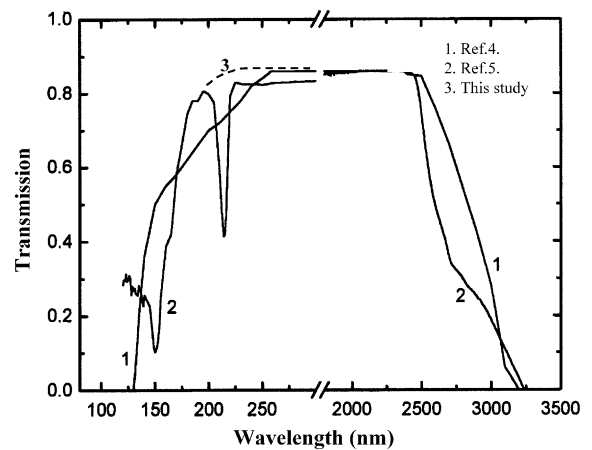


Fig. 4. Transparency of  $\text{SrB}_4\text{O}_7$  single crystal.

material [11]. These inclusions were derived from the supersaturation of impurities in the melt, and their entrapment occurred by the sudden rate of increase in cellular growth at the solid–liquid interface [11,12]. Thus, it was important to decrease those impurities and prevent cellular growth in order to grow transparent crystals. We also adjusted the stoichiometric composition by considering the content of volatile impurities, such as water, and maintained a high-temperature gradient to avoid cellular growth by changing the hot-zone structure. As a result, transparent SBO crystal was grown (Fig. 3). Although there were micro-cracks near the surface resembling a cloud, the crystal was transparent, and inclusions could not be observed under a microscope.

Transmission from 200 to 1100 nm using (010) polished plates ( $5 \times 5 \times 2 \text{ mm}^3$  and  $5 \times 5 \times 3 \text{ mm}^3$ ) and previous results are shown in Fig. 4. Plate transparency did not differ with thickness, and our results demonstrated high transmission rates and no absorption peak at 214 nm, compared with previous results. This may indicate that high-quality transparent crystal has been successfully grown and that the grown crystal will be suitable for SHG experiments in VUV. The dielectric anomaly in the temperature range of 300–750 K was not observed, demonstrating that SBO does not exhibit ferroelectric properties [13].

### 3.2. Growth of $\text{Sm}^{2+}:\text{SrB}_4\text{O}_7$ and its fluorescence properties

Fig. 5 depicts an as-grown  $\text{Sm}^{2+}:\text{SrB}_4\text{O}_7$  ( $\text{Sm}^{2+}:\text{SBO}$ ) crystal. The crystal was clouded by its polycrystalline structure as well as many cracks and voids. Grown crystals were identified with  $\text{SrB}_4\text{O}_7$  by X-ray diffraction. It is difficult to grow  $\text{Sm}^{2+}:\text{SBO}$  single crystals, but this should be considered further. Polished thin sections ( $3 \times 3 \times 1 \text{ mm}^3$ ) made from grown crystals are pinkish and transparent. The light pink coloring is caused by the incorporation of  $\text{Sm}^{2+}$  into the crystal. Fig. 6 illustrates the fluorescence spectra from 625 to 690 nm at 300 K of crystal, polycrystal and glass samples. The broad band  ${}^4\text{G}_{5/2} \rightarrow {}^6\text{H}_{9/2}$  transitions near 650 nm belongs to trivalent samarium, and the narrow line near 685 nm can be attributed to the  ${}^5\text{D}_0 \rightarrow {}^7\text{F}_0$  transitions of divalent samarium [10]. From this result, it may be considered that  $\text{Sm}^{3+}$  exists predominantly in a glass state and  $\text{Sm}^{2+}$  mainly in crystal and polycrystal, whereas  $\text{Sm}^{3+}$  and  $\text{Sm}^{2+}$  coexist in  $\text{Sm}:\text{SBO}$  ceramics prepared in air under the melting point [10]. Judging from these results,  $\text{Sm}^{3+}$  seems to be more stable in the melt. Thus, we conclude that a quantitative valence change from  $\text{Sm}^{3+}$  to  $\text{Sm}^{2+}$  takes place at the solid–liquid interface during growth. In the solid–liquid interface, its state is slightly reduced compared with the



Fig. 5. As-grown  $\text{Sm}^{2+}:\text{SrB}_4\text{O}_7$  crystal.

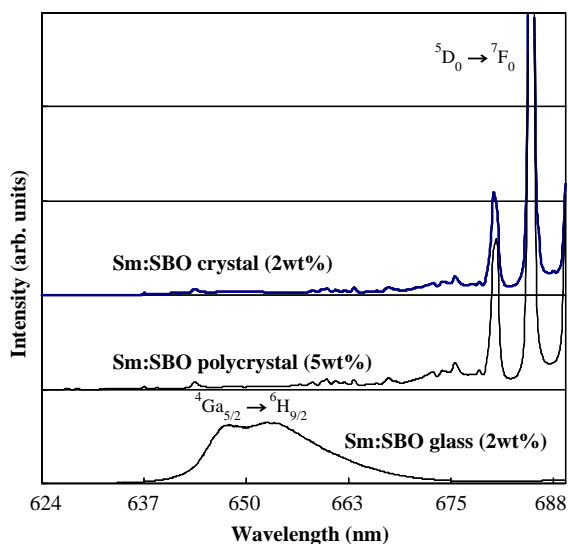


Fig. 6. Fluorescence spectra from 625 to 690 nm at 300 K of crystal, polycrystal and glass samples;  $\text{Sm}^{2+}:\text{SrB}_4\text{O}_7$  crystal was grown from the melt including 5 wt%  $\text{Sm}_2\text{O}_3$  and polycrystal and glass samples contain 5 and 2 wt%  $\text{Sm}_2\text{O}_3$ , respectively.

melt around the interface [11]. This reduced state is one reason for the result in the valence change of samarium.

X-ray diffraction patterns of grown crystals coincided with that of  $\text{SrB}_4\text{O}_7$ , although grown crystals include a small amount of Sm. This indicates that  $\text{Sm}^{2+}$  replaces the Sr site in SBO crystal. Fig. 7 illustrates the fluorescence spectra of 685.5 nm ( ${}^5\text{D}_0 \rightarrow {}^7\text{F}_0$  transition) of crystals, grown from the melt with 2 and 5 wt%  $\text{Sm}_2\text{O}_3$ . The content of Sm in each crystal was about 0.8 and 2.5 wt%  $\text{Sm}_2\text{O}_3$ , respectively. The fluorescence intensity was dependent upon the Sm content, and the intensity variation in crystal samples was almost undetectable. However, the fluorescence intensity and line width in  $\text{Sm}^{2+}:\text{SBO}$  polycrystal may fluctuate greatly, compared with the grown crystal. The reason for these differences is unclear; it is possible, however, that the concentration fluctuation of Sm due to rapid crystallization and other phase in the melt, and the strain of the crystal lattice due to the polycrystal structure, result in such differences. In addition,  $\text{Sm}^{2+}:\text{SBO}$  polycrystal contains  $\text{SrB}_6\text{O}_{10}$  as secondary phases and  $\text{SrB}_6\text{O}_{10}$  includes  $\text{Sm}^{2+}$ . The fluorescence

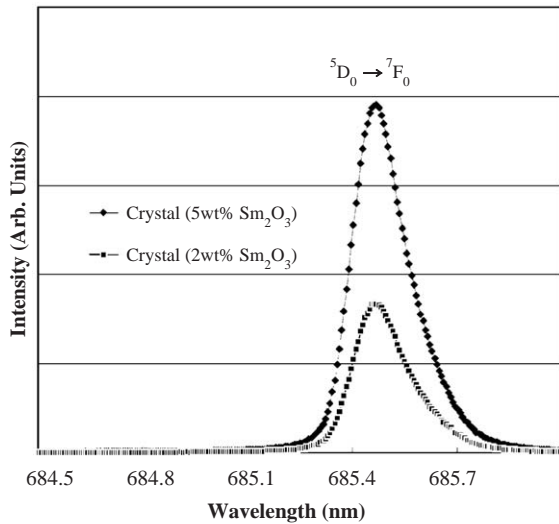


Fig. 7. Fluorescence spectra (685.5 nm) at room temperature of  $\text{Sm}^{2+}:\text{SrB}_4\text{O}_7$  crystal, grown from the melt with 2 and 5wt%  $\text{Sm}_2\text{O}_3$ , respectively.

spectra of  $^5\text{D}_0 \rightarrow ^7\text{F}_0$  transitions of divalent samarium in  $\text{SrB}_6\text{O}_{10}$  at room temperature overlap that in  $\text{Sm}^{2+}:\text{SBO}$  [14]. The pressure shift of this 0–0 emission line (685.5 nm) in  $\text{Sm}^{2+}:\text{SrB}_6\text{O}_{10}$ , however, is not the same as in  $\text{Sm}^{2+}:\text{SBO}$ . This makes the pressure measurement vague. Therefore, we conclude that crystal samples are more promising than  $\text{Sm}^{2+}:\text{SBO}$  polycrystal.

#### 4. Conclusions

A high-quality transparent SBO crystal was successfully grown by avoiding cellular growth and by reducing impurities, such as water and deviation from stoichiometric composition. The grown crystal showed high transmission and no absorption peak of 214 nm. SBO was the paraelectric material in the temperature range 300–750 K.

$\text{Sm}^{2+}$  exists predominantly in grown Sm:SBO crystals. The intensity fluctuation of 0–0 line was almost not observed in a thin section taken from

this crystal. This result demonstrates that  $\text{Sm}^{2+}:\text{SBO}$  crystal is promising as a pressure gauge material, and some earth science researchers have already confirmed pressures up to 40 GPa using this sample.

#### Acknowledgements

R. Komatsu thanks Electric Technology Research Foundation of Chugoku and Yamaguchi University Education and Research Foundation for financial supports.

#### Reference

- [1] K. Yamanouchi, H. Odagawa, T. Kojima, T. Matsumura, *Electron. Lett.* 33 (1997) 193.
- [2] P. Becker, *Borate Mater. Nonlinear Opt. Adv. Mater.* 10 (1998) 979.
- [3] Yu.S. Oseledchik, A.L. Prosvirnin, A.I. Pisarevskiy, V.V. Starshenko, V.V. Osadchuk, S.P. Belokrysov, N.V. Svitanko, A.S. Korol, S.A. Krikunov, A.F. Selevich, *Opt. Mater.* 4 (1995) 669.
- [4] Y.Yu.S. Oseledchik, A.L. Prosvirnin, V.V. Starshenko, V.V. Osadchuk, A.I. Pisarevsky, S.P. Belokrysov, A.S. Korol, N.V. Svitanko, A.F. Selevich, S.A. Krikunov, *J. Crystal Growth* 135 (1994) 373.
- [5] F. Pan, G. Shen, R. Wang, X. Wang, D. Shen, *J. Crystal Growth* 241 (2002) 108.
- [6] R. Komatsu, T. Suetsugu, S. Uda, M. Ono, *Ferroelectrics* 95 (1989) 103.
- [7] L. Bohaty, J. Liebertz, S. Staehr, *Z. Kristallogr.* 172 (1985) 135.
- [8] R. Komatsu and K. Ikeda, *Proceeding of 150th Committee on Acoustic Wave Device Technology 68th Technical meeting*, Vol. 1, 25 July 2000, (in Japanese with English abstract).
- [9] V. Petrov, F. Noack, D. Shen, F. Pan, G. Shen, X. Wang, R. Komatsu, *Opt. Lett.* 29 (4) (2004) 373.
- [10] P. Mikhail, J. Hulliger, M. Schnieper, H. Bill, *J. Mater. Chem.* 10 (2000) 987.
- [11] R. Komatsu, S. Uda, *Mater. Sci. Bull.* 33 (3) (1998) 433.
- [12] T. Sugawara, R. Komatsu, S. Uda, *J. Crystal Growth* 204 (1–2) (1999) 150.
- [13] Y. Akishige, R. Komatsu, in preparation.
- [14] H. Liang, Q. Zeng, T. Hu, S. Wang, Q. Su, *Solid State Sci.* 5 (2003) 465.